

Asymptotic Regulation of a One-Section Continuum Manipulator

Ian A. Gravagne

Baylor University, Waco, TX; Ian_Gravagne@baylor.edu

Abstract

Continuum manipulators are robotic manipulators built using one continuous, elastic, and highly deformable “backbone” instead of multiple rigid links connected by joints. This paper extends a previous control result for planar continuum robots by proposing a new asymptotic convergence argument for a PD-plus-feedforward controller. The benefit of the asymptotic arguments is that the backbone bending stiffness can be adaptively updated by the controller if it is not known a priori.

1 Introduction

“Continuum robots”, a phrase referenced from a survey paper by Robinson and Davies [1], refers to a class of robotic manipulators that essentially discard the traditional robot design paradigm that joins stiff, rigid links with rotational or prismatic joints. That this design methodology has been highly successful in the past is certainly not under debate; in fact, here and in previous work we suggest that rigid-link designs will continue to fulfill the majority of automation and manipulation need for the foreseeable future. However, rigid-link design and analysis seems to have reached some practical limits. Among these, it is difficult and often expensive to design compliance into a rigid-link robot at any point except the end-effector. We are beginning to see that compliance is a critical ingredient in the creation of safe, comfortable and interactive human-robot environments [2]. Compliance is also a significant asset for the manipulation or exploration of unknown or delicate environments, such as in a laparoscopic procedure, [3]. Additionally, rigid-link robots generally do not have the ability to use their entire structure to manipulate things, called “whole-arm manipulation”, and tend to be complex to build, heavy (in order to impart stiffness) and somewhat bulky.

Some of the aforementioned issues are being addressed by creative mechanical designs, which often accept some flexibility and vibration in the robot links in exchange for lighter weight, less complexity and greater safety margin.

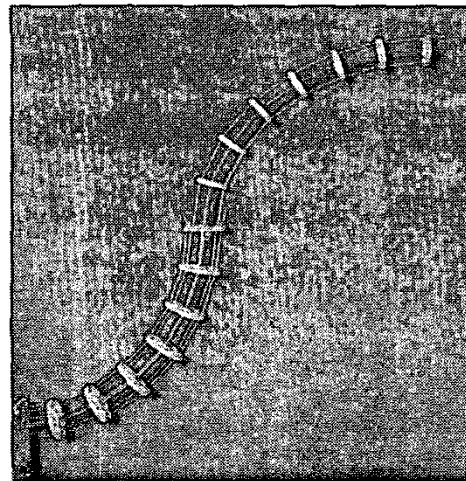


Figure 1: A two-section continuum robot adopts a typical pose.

Inspired by trunks, tentacles and snake backbones, continuum manipulators such as the simple prototype seen in figure 1 are among those designs. However, with new properties and capabilities, continuum robots also emphasize the need for new or expanded results in some areas that long ago matured for rigid-link robots. The author’s previous work established a basic but extremely important result in continuum manipulator control, namely, that a PD-plus-feedforward controller can exponentially regulate the position of a continuum robot [12] – a result long understood for rigid-link designs. The main drawback of that work was the dependence of the control law on exact knowledge of the “backbone” bending stiffness, a quantity that is difficult to measure. The objective of this paper, therefore, is to present an alternative (asymptotic) convergence argument for the PD-plus-feedforward controller, including an adaptive update law for the unknown stiffness term.

2 Background

The author's work in continuum manipulators grew out of the early studies of hyper-redundant and high-degree-of-freedom (HDOF) devices. Some of the initial HDOF design attempts appear in [4], [5] and [19]. More recent designs appear in [6] and [7], though this is certainly not an exhaustive list. For background into the kinematics and path-planning of continuum and hyper-redundant robots, see [8]-[10] and [14]-[17]. References [11]-[13] and [20] discuss the dynamics and control of continuum and hyper-redundant robots. Some of the fundamentals in this work are derived from the field of elastica mechanics, and details can be found in [18]-[23].

3 Dynamics and Control Law

The fundamental difference between a rigid-link robot and a continuum robot is that a continuum backbone exhibits infinite-dimensional kinematics and dynamics, described by differential and partial-differential equations, respectively. The added difficulty posed by such models often taxes the theoretical limits of our ability to analyze them. Making matters worse, any practically useful continuum robot with a sufficiently large workspace exhibits a range of deflection and bending far beyond what typical Euler-Bernoulli or other linear models can accurately reproduce, leaving only nonlinear large-deflection models for which there is precious little literature. (See [18] for an overview.) For these reasons, the work here is restricted for now to a planar model with a non-extensible backbone and negligible shear effects, such as the one pictured in figure 1.

While the previous control result illustrated in [12] focused on generating an exponential convergence result for backbones subject to multiple points of actuation (which are, of course, a necessary ingredient for any manipulator), the notational overhead somewhat obscured the most interesting points. Here, we will focus on the dynamics of one manipulator section, i.e. a span of flexible backbone actuated only at the unclamped end. The coordinate system is straightforward: the backbone centerline has length L ; any given point along the backbone is referenced from the origin through the arclength variable $s \in [0, L]$. At every point s and time t , the backbone has a Cartesian position $\underline{x}(s, t) = [x_1(s, t), x_2(s, t)]^T$ (underscores represent vector variables), as well as a tangent angle to the horizontal, $\theta(s, t)$. The backbone also experiences an internal shear/axial force field, $\underline{f}(s, t)$. The bending stiffness of a long, thin, elastic backbone is approximated by the constant EI (the product of Young's modulus and the

cross-section inertial density.); it also has rotational and translational inertial densities of I_ρ and ρ respectively, as well as a distributed damping coefficient b . Through cables or some other mechanism, a torque $\tau(t)$ is applied to the free end of the manipulator to bend it and cause a subsequent change in its end-effector position. Given these parameters and coordinates, the system dynamics follow as

$$-I_\rho \ddot{\theta} - b\dot{\theta} + \underline{q}^T S \underline{f} + EI\theta'' = 0 \quad (1a)$$

$$-\rho \ddot{\underline{x}} + \underline{f}' = \underline{0} \quad (1b)$$

$$\underline{x}' - \underline{q} = \underline{0} \quad (1c)$$

$$\theta(0, t) = 0 \quad (1d)$$

$$EI\theta'(L, t) = \tau \quad (1e)$$

$$\underline{x}(0, t) = \underline{0} \quad (1f)$$

$$\underline{f}(L, t) = \underline{0}. \quad (1g)$$

where $(\circ)' = \frac{d}{ds}$, $(\dot{\circ}) = \frac{d}{dt}$, and S and \underline{q} are given by

$$S = \begin{bmatrix} 0 & 1 \\ -1 & 0 \end{bmatrix}; \quad \underline{q} = \begin{bmatrix} \cos \theta \\ \sin \theta \end{bmatrix}. \quad (2)$$

The first two lines above represent the field dynamics, as a set of coupled nonlinear equations. The third line is the system kinematics, relating the tangent angle to the position. Boundary conditions (1d) and (1f) show that the manipulator is "clamped" and unmoving at the origin. Condition (1e) introduces the actuator torque, and condition (1g) suggests that the robot has no payload in, nor any actuators capable of exerting forces on, its end-effector. Note that the kinematics are often written in integral form,

$$\underline{x}(s, t) = \int_0^s \underline{q}(\sigma, t) d\sigma. \quad (3)$$

Canceling the time-derivative terms in (1a) leaves behind the backbone mechanics, the equations describing the static position of the backbone at rest. Quite simply, the backbone is predicted to take on a semi-circular shape, given by $EI\theta'' = 0$ (this can be seen in each section of the manipulator in figure 1.) Consequently, in attempting to drive the backbone into a desired shape $\theta_d(s)$, that shape must obey the static constraint that

$$\theta_d''(s) = 0 \quad (4)$$

otherwise it will be an unattainable control objective. Note the absence of the time variable above, since we are concerned with a regulation problem rather than a tracking problem. The backbone's elastic stiffness will necessitate a static "holding" torque, required to simply hold the

manipulator in a given pose. (This can be compared with the commonly used anti-gravity terms in many rigid-link robot controllers). In accordance with (1e), the holding torque must be equal to $EI\theta'_d(L)$. Thus, a reasonable and straightforward control law reads

$$\tau = EI\theta'_d(L) - k_d\dot{\theta}(s, t) - k_p\tilde{\theta}(s, t), \quad (5)$$

where $\tilde{\theta} = \theta(s, t) - \theta_d(s)$ is the shape error and k_d, k_p are positive control gains. This control law does, in fact, exponentially regulate the system dynamics to the desired static equilibrium [12]. However, it strictly depends on the positive constant EI , which may not be known. An alternate control law, the one of interest here, gives

$$\tau = \widehat{EI}\theta'_d(L) - k_d\dot{\theta}(L, t) - k_p\tilde{\theta}(L, t), \quad (6)$$

where \widehat{EI} is now a (time-varying) estimate of the true bending stiffness. It is updated according to the update law

$$\dot{\widehat{EI}} = -k\theta'_d(L) [\dot{\theta}(L, t) + \varepsilon \tanh \tilde{\theta}(L, t)] \quad (7)$$

where k and ε are positive constants, defined next. In essence, the update law above makes control law (6) similar to a PID controller. This can be seen by integrating (7) and observing that, near the origin, $\tanh \tilde{\theta}(L, t) \approx \tilde{\theta}(L, t)$. It is this "integral" behavior that drives the steady-state error to zero.

4 Asymptotic Regulation

The stability procedure begins by proposing a Lyapunov candidate

$$\begin{aligned} V &= V_1 + V_2, \\ V_1 &= \frac{1}{2} \int_0^L EI\tilde{\theta}'^2 + I_\rho\dot{\theta}^2 + \rho\dot{\underline{x}}^T\dot{\underline{x}}ds \\ &\quad + \frac{k_p}{2}\tilde{\theta}(L, t)^2 + \frac{1}{2k}\widehat{EI}^2 \\ V_2 &= \varepsilon \int_0^L I_\rho\dot{\theta} \tanh(\tilde{\theta}) + \rho \left[\int_0^s \tanh(\tilde{\theta})\underline{q}^T d\sigma \right] S\underline{x}ds, \end{aligned} \quad (8)$$

where $\widehat{EI} = \widehat{EI} - EI$. Clearly, V_1 is positive definite. V_2 (the "crossing function") may be negative, but the following arguments show that its absolute value is always less than V_1 for a sufficiently small choice of ε . For the first term in V_2 , note the standard inequality, $\int_a^b g^2 ds \leq$

$(b-a)^2 \int_a^b g'^2 ds$ if $g(a) = 0$. Thus,

$$\begin{aligned} &\left| \varepsilon \int_0^L I_\rho\dot{\theta} \tanh(\tilde{\theta}) ds \right| \\ &\leq \varepsilon \int_0^L I_\rho\dot{\theta}^2 + I_\rho \tanh^2(\tilde{\theta}) ds \\ &\leq \varepsilon \int_0^L I_\rho\dot{\theta}^2 + I_\rho\tilde{\theta}^2 ds \\ &\leq \varepsilon \int_0^L I_\rho\dot{\theta}^2 + I_\rho L^2\tilde{\theta}'^2 ds \end{aligned} \quad (11)$$

using another inequality, $ab \leq \gamma a^2 + \frac{1}{\gamma} b^2$ (with positive $\gamma = 1$ in this case). These inequalities arise frequently in work of this nature, [21]. The second term yields

$$\begin{aligned} &\left| \varepsilon \int_0^L \rho \left[\int_0^s \tanh(\tilde{\theta})\underline{q}^T d\sigma \right] S\underline{x}ds \right| \\ &\leq \varepsilon \int_0^L \rho\dot{\underline{x}}^T S^T S\underline{x} \\ &\quad + \rho \left[\int_0^s \tanh(\tilde{\theta})\underline{q}^T d\sigma \right] \left[\int_0^s \tanh(\tilde{\theta})\underline{q} d\sigma \right] ds \\ &\leq \varepsilon \int_0^L \rho\dot{\underline{x}}^T\dot{\underline{x}} + \rho s^2 \tanh^2(\tilde{\theta})\underline{q}^T\underline{q} ds \\ &\leq \varepsilon \int_0^L \rho\dot{\underline{x}}^T\dot{\underline{x}} + \rho L^2\tilde{\theta}^2 ds \\ &\leq \varepsilon \int_0^L \rho\dot{\underline{x}}^T\dot{\underline{x}} + \rho L^4\tilde{\theta}'^2 ds. \end{aligned} \quad (12)$$

Combining (11) and (12) gives

$$|V_2| \leq \varepsilon \int_0^L I_\rho\dot{\theta}^2 + \rho\dot{\underline{x}}^T\dot{\underline{x}} + L^2(I_\rho + L^2\rho)\tilde{\theta}^2 ds, \quad (13)$$

(8) guaranteeing that $V > 0$ if

$$\varepsilon < \min \left\{ 1, \frac{EI}{L^2(I_\rho + L^2\rho)} \right\}. \quad (14)$$

Choosing such an ε furthermore ensures that V is radially unbounded.

The time derivative of V_1 follows directly as

$$\dot{V}_1 = \int_0^L -b\dot{\theta}^2 ds - k_d\dot{\theta}(L, t)^2 + \widehat{EI} \left[\theta'_d(L)\dot{\theta}(L, t) + \frac{\dot{\widehat{EI}}}{k} \right]. \quad (15)$$

The time derivative of V_2 , after substitution of the dynam-

ics, integration by parts and some cancellation, gives

$$\begin{aligned} \dot{V}_2 &= \int_0^L g I_\rho \dot{\theta}^2 + \tanh(\tilde{\theta}) \left[-b\dot{\theta} + EI\theta'' \right] \\ &+ \rho \left[\int_0^s g \dot{\theta} \underline{q}^T S - \tanh(\tilde{\theta}) \dot{\theta} \underline{q}^T d\sigma \right] \dot{\underline{x}} ds, \end{aligned} \quad (16)$$

where $g(s, t) \triangleq 1 - \tanh^2(\tilde{\theta})$. The expression above contains five terms, and the following analysis deals with the last four of those. For the second term, note that $g \leq 1$, implying that $g^2 \leq g$. Thus,

$$\begin{aligned} \int_0^L -b\dot{\theta} \tanh(\tilde{\theta}) ds &\leq \int_0^L \frac{b}{\gamma} \dot{\theta}^2 + b\gamma \tanh^2(\tilde{\theta}) ds \\ &\leq \int_0^L \frac{b}{\gamma} \dot{\theta}^2 + b\gamma L^2 \tanh^2(\tilde{\theta}) ds \\ &= \int_0^L \frac{b}{\gamma} \dot{\theta}^2 + b\gamma L^2 g^2 \tilde{\theta}^2 ds \\ &\leq \int_0^L \frac{b}{\gamma} \dot{\theta}^2 + b\gamma L^2 g \tilde{\theta}^2 ds. \end{aligned} \quad (17)$$

Examining the third term yields (18) [next page]. In line 4 of (18), recall that $\theta_d'' = 0$. In the last line of (18), we may employ another inequality, $g^2 \leq |b-a| \int_a^b g'^2 ds$, to see that

$$\begin{aligned} &-k_d \dot{\theta}(L, t) \tanh \tilde{\theta}(L, t) \\ &\leq \frac{k_d}{\beta} \dot{\theta}(L, t)^2 + k_d \beta \tanh^2 \tilde{\theta}(L, t) \\ &\leq \frac{k_d}{\beta} \dot{\theta}(L, t)^2 + k_d \beta L \int_0^L \tanh^2 \tilde{\theta} ds \\ &\leq \frac{k_d}{\beta} \dot{\theta}(L, t)^2 + k_d \beta L \int_0^L g \tilde{\theta}^2 ds. \end{aligned} \quad (19)$$

Moving on, we may bound term 4 of (16) by

$$\begin{aligned} &\int_0^L \rho \left[\int_0^s g \dot{\theta} \underline{q}^T S d\sigma \right] \dot{\underline{x}} ds \\ &\leq \sup_{s,t} (g) \left| \int_0^L \rho \left[\int_0^s \dot{\theta} \underline{q}^T S d\sigma \right] \dot{\underline{x}} ds \right| \\ &= \int_0^L \rho \left[\int_0^s \dot{\theta} \underline{q}^T S d\sigma \right] \left[\int_0^s \dot{\theta} S^T \underline{q} d\sigma \right] ds \\ &\leq \int_0^L \rho L^2 \left[\dot{\theta} \underline{q}^T S \right] \left[\dot{\theta} S^T \underline{q} \right] ds = \int_0^L \rho L^2 \dot{\theta}^2 ds \end{aligned} \quad (20)$$

noticing that $\dot{\underline{x}}$ is given by differentiating (3). Lastly, term

5 of (16) is bounded by the following argument:

$$\begin{aligned} &\int_0^L \rho \left[\int_0^s -\tanh(\tilde{\theta}) \dot{\theta} \underline{q}^T d\sigma \right] \dot{\underline{x}} ds \\ &= -\int_0^L \rho \left[\int_0^s \tanh(\tilde{\theta}) \dot{\theta} \underline{q}^T d\sigma \right] \left[\int_0^s \dot{\theta} S^T \underline{q} d\sigma \right] ds \\ &\leq \rho \left(\int_0^L \left\| \int_0^s \tanh(\tilde{\theta}) \dot{\theta} \underline{q}^T d\sigma \right\|^2 ds \int_0^L \left\| \int_0^s \dot{\theta} S^T \underline{q} d\sigma \right\|^2 ds \right)^{\frac{1}{2}} \\ &\leq \rho \left(\int_0^L L^2 \left\| \tanh(\tilde{\theta}) \dot{\theta} \underline{q}^T \right\|^2 ds \int_0^L L^2 \left\| \dot{\theta} S^T \underline{q} \right\|^2 ds \right)^{\frac{1}{2}} \\ &\leq \rho \left(\int_0^L L^2 \tanh^2(\tilde{\theta}) \dot{\theta}^2 ds \int_0^L L^2 \dot{\theta}^2 ds \right)^{\frac{1}{2}} \leq \int_0^L \rho L^2 \dot{\theta}^2 ds, \end{aligned} \quad (21)$$

where the Cauchy-Schwarz inequality was used. Compiling (17), (18), (19), (20) and (21) along with \dot{V}_1 then gives

$$\begin{aligned} \dot{V} &= \int_0^L - \left[b - \varepsilon \left(g I_\rho + 2\rho L^2 + \frac{b}{\gamma} \right) \right] \dot{\theta}^2 \\ &- \varepsilon g \left[EI - \gamma b L^2 - k_d \beta L \right] \tilde{\theta}^2 ds \\ &- \varepsilon k_p \tilde{\theta}(L, t) \tanh \tilde{\theta}(L, t) - \left[k_p - \varepsilon \frac{k_d}{\beta} \right] \dot{\theta}(L, t)^2 \\ &+ \widetilde{EI} \left[\theta'_d(L) \dot{\theta}(L, t) + \frac{\widetilde{EI}}{k} + \varepsilon \theta'_d(L) \tanh \tilde{\theta}(L) \right]. \end{aligned} \quad (22)$$

Substituting in the bending stiffness update law eliminates the last line above, leaving \dot{V} a negative quantity in all states except \widetilde{EI} , assuming sufficiently small choices of positive constants β , γ and ε .

Using an invariance argument, we now assume that $\dot{V} = 0$ for all future times. It directly follows that $\int_0^L \tilde{\theta}^2 ds = 0$, and thus (using an inequality described earlier) that $\tilde{\theta}(s, t) = 0$ as well as $\tilde{\theta}'(s, t) = 0$. Picking $s = L$, we have $\dot{\theta}(L, t) = \tilde{\theta}(L, t) = \tilde{\theta}'(L, t) = 0$, which forces (1e) and (6) to yield

$$\widetilde{EI} = 0, \quad (23)$$

illustrating that update law (7) guarantees convergence of \widetilde{EI} to its true value.

5 Simulation and Conclusions

The main drawback of (7) is its dependence on ε , which is limited to an upper bound of one under the best of conditions, much less than one in general. This results in a very slow convergence for \widetilde{EI} because, even if k is raised, the

$$\begin{aligned}
\int_0^L \tanh(\tilde{\theta}) EI \tilde{\theta}'' ds &= \int_0^L -\tanh'(\tilde{\theta}) EI \tilde{\theta}' ds + EI \tilde{\theta}'(L, t) \tanh \tilde{\theta}(L, t) \\
&= \int_0^L -\tanh'(\tilde{\theta}) EI \tilde{\theta}' ds + \left[\widetilde{EI} \theta'_d(L) - k_d \dot{\theta}(L, t) - k_p \tilde{\theta}(L, t) \right] \tanh \tilde{\theta}(L, t) \\
&= \int_0^L -\tanh'(\tilde{\theta}) EI (\tilde{\theta}' + \theta'_d) ds + \left[(\widetilde{EI} + EI) \theta'_d(L) - k_d \dot{\theta}(L, t) - k_p \tilde{\theta}(L, t) \right] \tanh \tilde{\theta}(L, t) \\
&= \int_0^L -\tanh'(\tilde{\theta}) EI \tilde{\theta}' + \tanh(\tilde{\theta}) EI \theta''_d ds + \left[\widetilde{EI} \theta'_d(L) - k_d \dot{\theta}(L, t) - k_p \tilde{\theta}(L, t) \right] \tanh \tilde{\theta}(L, t) \\
&= \int_0^L -g EI \tilde{\theta}^2 ds + \widetilde{EI} \theta'_d(L) \tanh \tilde{\theta}(L, t) - k_d \dot{\theta}(L, t) \tanh \tilde{\theta}(L, t) - k_p \tilde{\theta}(L, t) \tanh \tilde{\theta}(L, t).
\end{aligned} \tag{18}$$

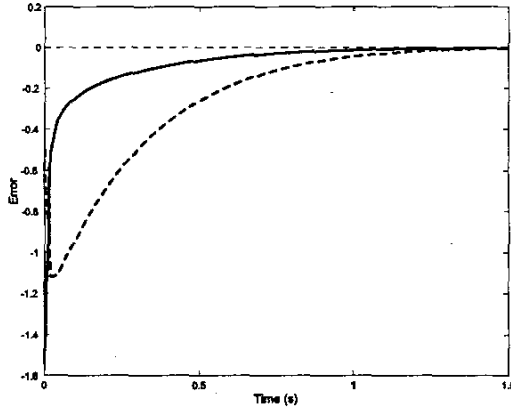


Figure 2: Step response errors $\tilde{\theta}(L, t)$ (solid line) and \widetilde{EI} (dashed line). The update law uses $k = 0.5$ and $\varepsilon = 10$. Smaller ε simply results in slower convergence.

update algorithm must wait for $\dot{\theta}(L, t)$ to become “small enough” that the ε term can be effective. There does not seem to be any algorithmic reason why ε cannot be made arbitrarily high in (7), and introducing a separate gain for the ε term of (7) would be a good improvement over the current update law. The simulation results in figures 2 and 3 show that faster convergence is possible.

To summarize, this paper presents a new asymptotic stability and convergence argument for continuum elastica manipulators under “PD-plus-feedforward” control, including an adaptive update rule for the unknown bending stiffness. Future work on this topic should include introduction of the effects of multiple actuators on the backbone, as well as experimental verification that the proposed update law works. Also, though somewhat of a

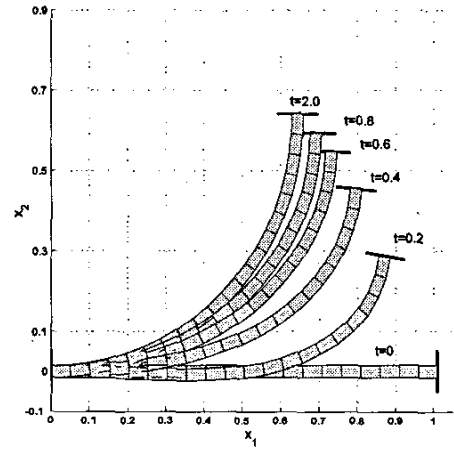


Figure 3: A time-lapse image of the one-section manipulator moving to the desired shape $\theta_d(s) = s\pi/2$. System constants are scaled to realistic ratios: $EI = 1$, $\rho = 0.7$, $I_\rho = 0.001$. Gains $k_d = 0$ and $k_p = 20$.

technicality, invariance arguments for infinite-dimensional systems require proof of the existence of solutions to the dynamical equations, a step not taken here. Long-term improvements might include the incorporation of more accurate damping models [25] and an extension of the work to the three-dimensional domain.

References

- [1] G. Robinson and J.B.C. Davies, “Continuum Robots – A State of the Art,” Proc. IEEE Int. Conf. Robotics and

- Automation, Detroit, MI, May 1999, pp. 2849-2854
- [2] H. Lim, K. Tanie, "Human Safety Mechanisms of Human-Friendly Robots: Passive Viscoelastic Trunk and Passively Movable Base," *Int'l Journal of Robotics Research*, vol. 19, No. 4, April 2000, pp. 307-335
- [3] W.M. Aguilera, M.I. Frecker, "Design and Modeling of an Active Steerable End-Effector," *Proc. Smart Structures and Materials 2001*, pp. 490-498
- [4] S. Hirose, *Biologically Inspired Robots*. Oxford University Press, 1993
- [5] V.C. Anderson and R.C. Horn, "Tensor Arm Manipulator Design," *American Society of Mechanical Engineers*, paper #67-DE-57, 1967
- [6] R. Cieslak and A. Morecki, "Elephant Trunk Type Elastic Manipulator - a Tool for Bulk and Liquid Materials Transportation," *Robotica*, 1999, vol. 17 pp. 11-16
- [7] H. Tsukagoshi, A. Kitagawa, M. Segawa, "Active Hose: An Artificial Elephant's Nose with Maneuverability for Rescue Operation," *Proc. IEEE Int. Conf. on Robotics and Automation (ICRA)*, Seoul, Korea, May 2001, pp. 2454-2459
- [8] I. Gravagne and I.D. Walker, "Kinematic Transformations for Remotely-Actuated Planar Continuum Robots," *Proc. IEEE Int. Conf. on Robotics and Automation (ICRA)*, San Francisco, May 2000, pp. 19-26
- [9] I. Gravagne and I.D. Walker, "On the Kinematics of Remotely-Actuated Continuum Robots," *Proc. IEEE Int. Conf. on Robotics and Automation (ICRA)*, San Francisco, May 2000, pp. 2544-2550
- [10] I. Gravagne and I.D. Walker, "Manipulability, Force and Compliance Analysis for Planar Continuum Manipulators," *IEEE Trans. Robotics and Automation*, vol. 18, no. 3, June 2002, pp. 263-273
- [11] I. Gravagne, C.D. Rahn and I.D. Walker, "Large Deflection Dynamics and Control for Planar Continuum Robots," to appear, *ASME/IEEE Transaction on Mechatronics*
- [12] I. Gravagne and I.D. Walker, "Uniform Regulation of a Multi-Section Continuum Manipulator," *Proc. IEEE Int. Conf. Robotics and Automation*, Washington D.C., May 2002, pp. 1519-1524.
- [13] M. Ivanescu, "Position Dynamic Control for a Tentacle Manipulator," *Proc. IEEE Int. Conf. Robotics and Automation*, Washington D.C., May 2002, pp. 1531-1538.
- [14] I.D. Walker and M.W. Hannan, "A Novel Elephant's Trunk Robot", *Proc. IEEE/ASME Intl. Conf. on Advanced Intelligent Mechatronics*, Atlanta, GA, Sept. 1999, pp. 410-415
- [15] M. Hannan and I.D. Walker, "Novel Kinematics for Continuum Robots," *7th Int'l Symposium on Advances in Robot Kinematics*, Piran, Slovenia, June 2000, pp. 227-238
- [16] M. Hannan and I.D. Walker, "Analysis and Initial Experiments for a Novel Elephant's Trunk Robot," *Proc. IEEE/RSJ Int. Conf. on Intelligent Robots and Systems (IROS)*, Takamatsu, Japan, November 2000, pp. 330-337
- [17] G.S. Chirikjian, "Theory and Applications of Hyper-Redundant Robotic Manipulators," Ph.D. thesis, Dept. of Applied Mechanics, California Institute of Technology, June, 1992
- [18] J.C. Simo, L. Vu-Quoc, "On the Dynamics of Flexible Beams under Large Overall Motions - The Plane Case," *Journal of Applied Mechanics*, vol. 53, December 1986, pp. 849-863
- [19] S. Ma, S. Hirose, and H. Yoshinada, "Design and Experiments for a Coupled Tendon-driven Manipulator," *IEEE Control Systems Magazine*, vol. 13, no. 1, 1993, pp. 30-36
- [20] S. Ma, I. Kobayashi, S. Hirose, and K. Yokoshima, "Control of a Multijoint Manipulator: Moray Arm," *IEEE/ASME Trans. on Mechatronics*, vol. 7, no.3, 2002, pp. 304-317
- [21] C.D. Rahn, *Mechatronic Control of Distributed Vibration and Noise*, Berlin: Germany, Springer-Verlag, 2001.
- [22] J.G. Easley, *Mechanics of Elastic Structures*, Prentice Hall, Englewood Cliffs, NJ, 1989.
- [23] E.H. Love, *A Treatise on the Mathematical Theory of Elasticity*, Dover Publications, NY, 1944
- [24] K. Ito, "Uniform Stabilization of the Dynamic Elastica by Boundary Feedback," *SIAM J. Control Optim.*, vol. 37, no. 1, 1998, pp. 316-329
- [25] H.T. Banks, D.J. Inman, "On Damping Mechanisms in Beams," *Transactions of the ASME*, vol. 58, September 1991, pp. 716-723.